

FAST REVERSIBLE NiTi FIBERS FOR USE IN MICROBOTICS

Ian W. Hunter, Serge Lafontaine, John M. Hollerbach and Peter J. Hunter
Biorobotics Laboratory, Department of Biomedical Engineering,
McGill University, 3775 University Street, Montreal, Canada H3A 2B4

ABSTRACT

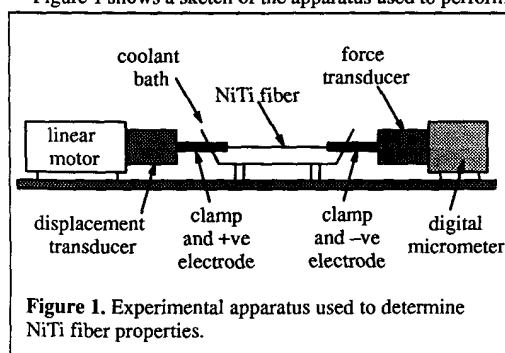
We report the experimentally determined characteristics of NiTi fibers which have been modified using a preparation procedure in which the fibers were subjected to brief very large current pulses during forced stretching. The modified fibers contract and relax fast enough to be of use in micro-robotics. The modified fibers generate a maximum extrapolated stress of 230 MN/m^2 and yield a peak measured power/mass approaching 50 kW/kg . The theory of a micro-actuator incorporating the modified fibers is presented.

INTRODUCTION

The shape memory alloy NiTi generates large forces ($>100 \text{ MN/m}^2$) with substantial displacements (up to 10% strain), and appears to hold considerable promise as an actuator either in fiber form in robotics [1] or in thin film form in micro-mechanics [2][3][4]. Two drawbacks that have limited the usefulness of NiTi actuators are (1) low bandwidth (around 1 Hz in fiber form [1] and 5 Hz in thin film form [4]) and (2) nonlinear dynamics. The low bandwidth is due to the long relaxation time which is usually assumed to be determined by the relatively long cooling thermal time constant.

EXPERIMENTAL APPARATUS

Figure 1 shows a sketch of the apparatus used to perform



mechanical experiments on the NiTi fibers. A NiTi fiber is clamped between a force transducer at one end and a linear motor and displacement transducer at the other end. The displacement transducer was a lateral effect photodiode with a flat bandwidth to 1 kHz. The force transducer was a strain

gaged proving ring with a flat bandwidth to 1 kHz. External forces were applied using a servo-controlled electromagnetic linear (voice-coil) motor. The NiTi fibers were immersed in recirculating methanol which was stirred and cooled to -10°C . All experiments were under computer control and force and displacement data were sampled via 12 bit A/Ds. The NiTi fibers were subjected to either sustained constant currents or computer controlled current pulses delivered using 200 A power-MOSFETS.

NiTi Fiber Modification

Figure 2 shows the contraction of a 100 mm long 0.8 mm

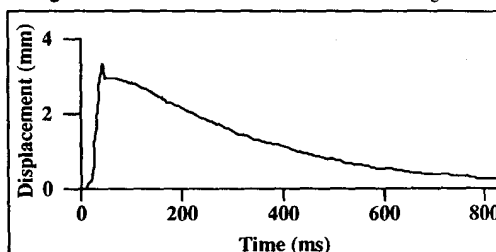


Figure 2. Change in length of a 0.8 mm diameter 100 mm long NiTi fiber following a brief current pulse.

diameter NiTi fiber following a single brief current pulse. The relaxation back to its original length is slow compared with the contraction time. Indeed in robotic applications the time taken to relax is usually much longer than this because cooling conditions were very favorable here. We tried a variety of cooling methods including vortex cooling and Peltier effect heat pumps without significant improvements.

We have attempted to shorten the relaxation time and have found that by exposing NiTi fibers to very large brief current pulses ($> 10^9 \text{ A/m}^2$ which may be generated for example using 2000 A radar thyristers) during externally imposed shortening and lengthening cycles we can change their properties. The altered NiTi now will both shorten and lengthen very rapidly as shown in Figure 3. The time course of this twitch response is shown in more detail in Figure 4. It is unclear to us why the relaxation time has changed so dramatically. It could be that the material properties have been altered in some way and/or that mechanical recoil via the NiTi stiffness is involved.

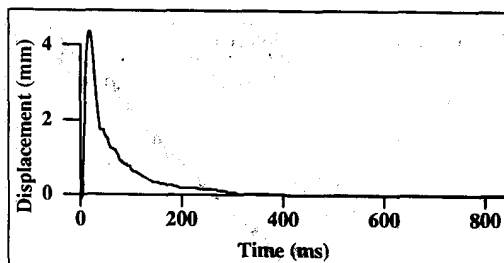


Figure 3. Change in length of 100 mm long modified NiTi fiber following a brief current pulse.

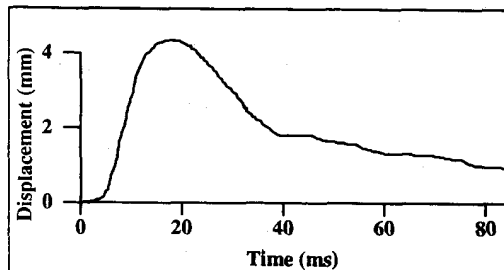


Figure 4. Change in length of 100 mm long modified NiTi fiber following a brief current pulse.

CHARACTERISTICS

We now present the result of experiments performed to characterize the mechanical properties of the modified NiTi fibers.

Force

When the modified NiTi fibers are subjected to a constant load (via the linear motor) they produce a peak force which if greater than the imposed load causes shortening. The difference between the peak force generated and the imposed load (i.e., incremental stress) is a function of the imposed load (i.e., applied stress) as shown in Figure 5. This figure also shows that the linear extrapolated force at which the load force equals the force generated (i.e., incremental force is zero) corresponds to a stress of 235 MN/m². For comparison the peak stress generated by human skeletal muscle is about 350 kN/m².

Power/Mass

The peak power/mass of these modified NiTi fibers is a function of externally imposed stress as shown in Figure 6. When loaded to a stress of 100 MN/m² the modified fibers produce a power/mass of nearly 50 kW/kg. For comparison the peak power/mass generated by human skeletal muscle is about 200 W/kg (about 50 W/kg sustained).

% Contraction

When heated with constant amplitude and duration current pulses the maximum shortening strain achieved by the

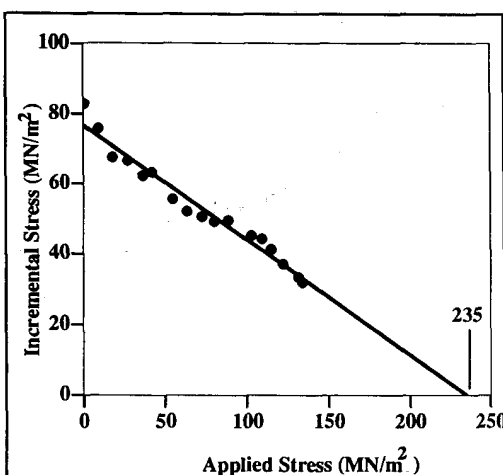


Figure 5. Externally applied stress to incremental stress generated by modified NiTi fiber.

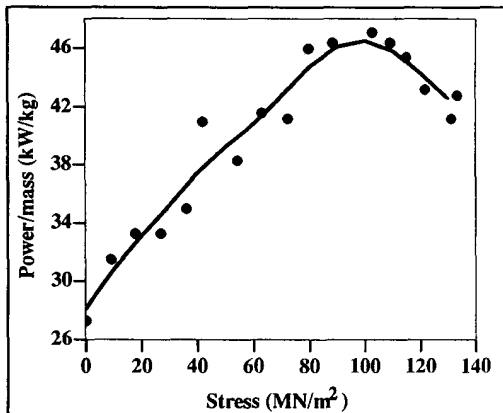


Figure 6. Peak power/mass of modified NiTi fiber.

modified fibers is a function of externally imposed stress as shown in Figure 7. Note that even with a load of 100 MN/m² the fibers shorten by over 1%.

Shortening Velocity

The strain rate (shortening velocity) is a monotonically decreasing function of load as shown in Figure 8. Note that at zero imposed load the strain rate is 3 s⁻¹ and even with an imposed load of 100 MN/m² is still 1 s⁻¹.

Comparisons

Hence it now appears that NiTi can be made fast enough as a macro or micro actuator, with impressive force/mass and power/mass ratios. Figure 9 shows a comparison of the power/mass of nature's actuator muscle, modified NiTi and a range of aircraft internal combustion engines. The modified NiTi has a peak power/mass about 100 times greater than muscle. However the comparison does not take into consider-

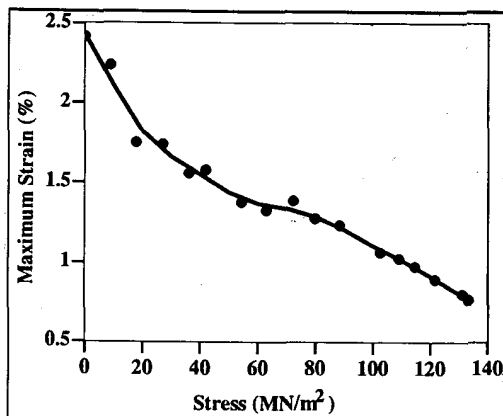


Figure 7. Maximum shortening (strain) of modified NiTi fiber as a function of externally applied stress.

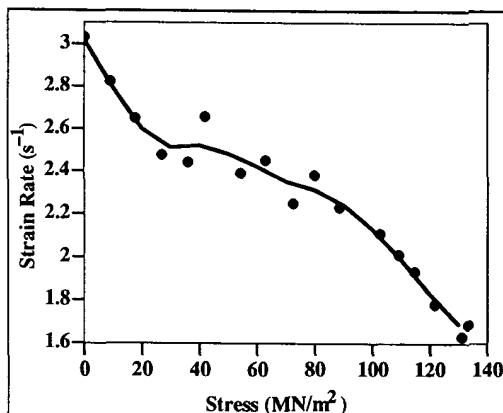


Figure 8. Peak shortening velocity (strain rate) of modified NiTi fiber as a function of stress generated.

ation the mass of the cooling system surrounding the NiTi fiber. When this is done both the peak stress generated and power/mass of muscle and modified NiTi are similar.

The Table shows a comparison of some properties of modified NiTi and muscle (human skeletal). It is important to remember that some of the values for the NiTi shown in the Table will be considerably less when the mass and volume of the cooling system is included.

NONLINEAR PROPERTIES AND CONTROL

The electromechanical properties of the NiTi fibers are dynamically nonlinear and time-varying [10]. For effective control of the fibers for fast movements we have found that it is necessary to characterize these properties experimentally using nonlinear time-varying system identification techniques. These techniques [6,7] also hold considerable promise for use in characterizing the properties of other micro-actuator technologies.

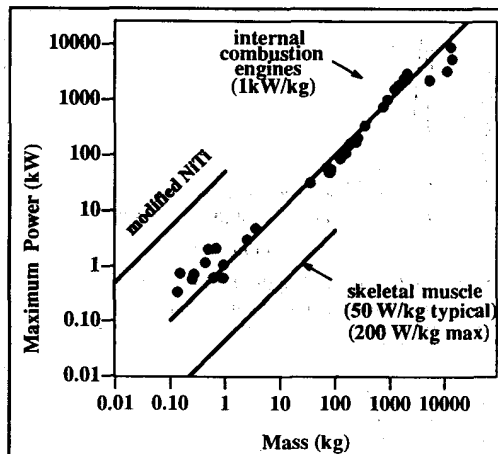


Figure 9. The peak powers produced by modified NiTi fibers, a range of aircraft internal combustion engines and human muscle.

Table: Comparison of Modified NiTi and Muscle

	NiTi	Muscle
Maximum tension (kN/m²)	>200,000	350
Maximum power/mass (W/kg)	>30,000	<500
Maximum strain rate (s⁻¹)	>3	<2
Typical max. displacement (%)	5	20
Power efficiency (%)	>1	>35

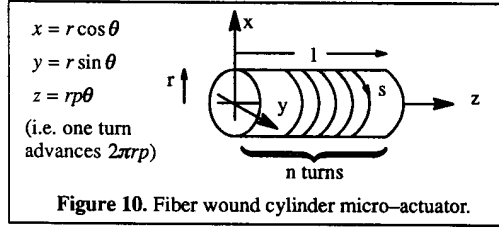
Various control schemes have been used to control NiTi fibers [8,9,10]. When forces larger than a single fiber can produce must be generated the NiTi fiber are arranged in parallel mechanically. When this is done we have found that a combination of pulse rate modulation and recruitment of fibers may be used to control force. This same scheme is used in nature in the neuromuscular control of whole muscle (muscle fiber bundles) force. Indeed for high bandwidth applications any single NiTi fiber should not be restimulated for a few hundred milliseconds to enable it to fully recover to its original state (see Figure 4 where it may be observed that the fiber rapidly lengthens only by about 2/3 and then for the remaining 1/3 recovers more slowly).

CONTRACTION OF FIBRE WOUND CYLINDER

We now consider a microactuator design which can make use of the properties of the modified NiTi fibers. We propose using small controlled length changes of the NiTi fibers to produce a large displacement, large force microactuator as follows. The NiTi fiber is wound around a cylindrical tube of length l , radius r and constant volume

$$V = \pi r^2 l \quad (1)$$

as shown in Figure 10. If the pitch of the helix is p , one turn



corresponds to an axial distance of $2\pi rp$, and the length for n turns is

$$l = rpn2\pi \quad (2)$$

The length of fibre in one turn is

$$s = \int_0^{2\pi} \sqrt{dx^2 + dy^2 + dz^2} = r \int_0^{2\pi} \sqrt{1 + p^2} d\theta = 2\pi r \sqrt{1 + p^2} \quad (3)$$

using the rectangular cartesian coordinates $x = r \cos \theta$, $y = r \sin \theta$ and $z = rp\theta$ shown in Figure 10.

From Equation 1, with V constant,

$$\frac{dl}{dr} = -\frac{2V}{\pi r^3} \quad (4)$$

and from Equations 1 and 2

$$p = \frac{V}{2n\pi^2 r^3} \quad (5)$$

The rate of change of cylinder length l with respect to radius r is

$$\frac{dl}{ds} = \frac{dl}{dr} \cdot \frac{dr}{ds} = -\frac{\frac{2V}{\pi r^3}}{\frac{ds}{dr}} \quad (6)$$

where, from Equations 2 and 3,

$$\frac{ds}{dr} = \frac{\partial s}{\partial r} + \frac{\partial s}{\partial p} \frac{dp}{dr} = 2\pi \sqrt{1 + p^2} + \frac{2\pi rp}{\sqrt{1 + p^2}} \cdot \frac{dp}{dr}$$

$$\text{where } \frac{dp}{dr} = -\frac{3V}{2n\pi^2 r^4} = -\frac{3p}{r}$$

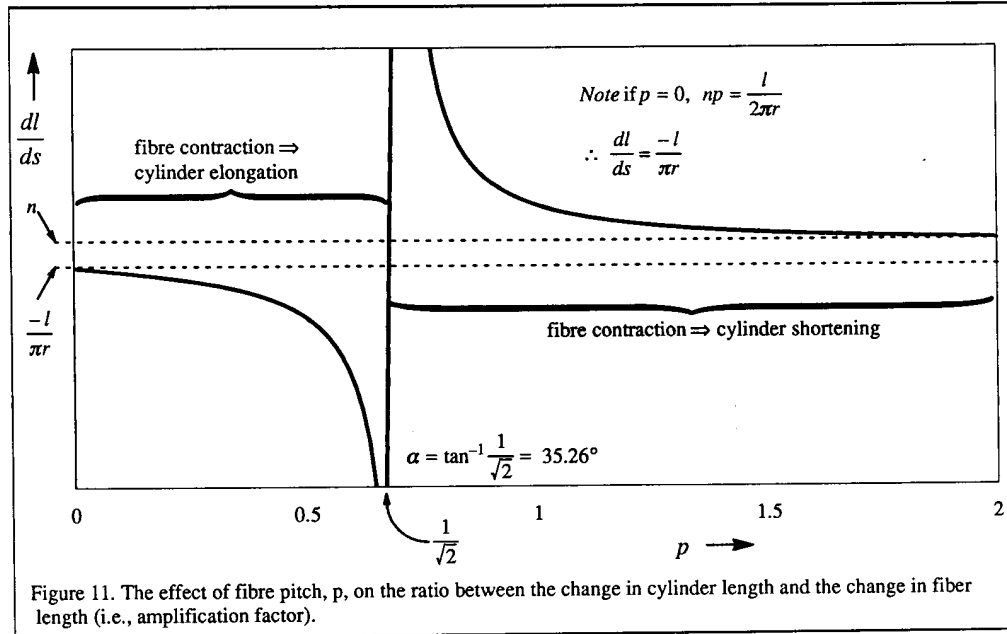
gives

$$\frac{ds}{dr} = 2\pi \left[\sqrt{1 + p^2} - \frac{3p^2}{\sqrt{1 + p^2}} \right] = 2\pi \frac{1 - 2p^2}{\sqrt{1 + p^2}}$$

and hence Equation 6 becomes

$$\frac{dl}{ds} = -\frac{2V}{\pi r^3} \cdot \frac{\sqrt{1 + p^2}}{2\pi(1 - 2p^2)} = -2np \frac{\sqrt{1 + p^2}}{1 - 2p^2} \quad (7)$$

This relationship is plotted in Figure 11, which shows the singular behavior occurring at $p = \frac{1}{\sqrt{2}}$.



For a given constant volume V , fiber-turn length s , and number of turns n , the radius, length and pitch of the cylinder can be calculated as follows: From Equations 1, 3 and 5

$$r^3 = \left(\frac{s}{2\pi\sqrt{1+p^2}} \right)^3 = \frac{V}{2n\pi^2 p}$$

gives

$$nps^3 = 4\pi(1+p^2)^{\frac{3}{2}}V \quad (8)$$

Putting $p = \tan \alpha$, where α is the angle subtended by the tangent to the fiber in the circumferential direction, Equation 8 becomes

$$(1+p^2)^{\frac{3}{2}} = \sec^3 \alpha$$

and Equation 8 becomes

$$ns^3 \tan \alpha = 4\pi \sec^3 \alpha V \quad \text{or} \quad \sin \alpha \cos^2 \alpha = \frac{4\pi V}{ns^3}$$

Now if we put $\sin \alpha = x$

$$x - x^3 = \frac{4\pi V}{ns^3}$$

or

$$x^3 - x + a = 0 \quad \text{where} \quad a = \frac{4\pi V}{ns^3}$$

Solving this cubic equation for x yields the pitch p , for a given volume V and fiber length s . The cylinder radius and length then follow from Equations 2 and 3.

At $p = \frac{1}{\sqrt{2}}$, corresponding to the fiber making an angle $\alpha = \tan^{-1} p = 35.26^\circ$ with the circumferential direction, the fiber length s , is a minimum and the rate of cylindrical length change with fiber length change is infinite (here we are considering kinematics only – of course the forces required to achieve this length change would be correspondingly large). When the pitch is less than this critical value contraction of the fiber causes the cylinder to lengthen and the pitch to increase. Similarly, for an initial pitch greater than the critical value, fiber contraction leads to cylinder contraction or fiber lengthening to cylinder lengthening. Thus, by suitably adjusting the shape of the cylinder and hence the initial pitch prior to controlled fiber contraction or lengthening, the cylinder

length can be controlled with a desired mechanical amplification factor.

ACKNOWLEDGEMENTS

This work was partly supported by the Natural Sciences and Engineering Research Council of Canada (NSERC) through the Strategic Grant STR-0040872. Personal support for IWH was provided by a Canadian Institute for Advanced Research (CIAR)/General Motors (GM) Fellowship and for JMH by an NSERC/CIAR Industrial Research Chair.

REFERENCES

- [1] Bergamasco, M., Salsedo, F. and Dario, P. A linear SMA motor as direct-drive robotic actuator. *Proc. IEEE Int. Conf. on Robotics and Automation*, 1989, 1, 618–623.
- [2] Ikuta, K., Fujita, H., Ikeda, M. and Yamashita, S. Crystallographic analysis of TiNi shape memory alloy thin film for micro actuator. *Proc. IEEE Micro Electro Mechanical Systems*, Napa Valley, CA, Feb. 11–14, 1990, pp. 38–39.
- [3] Busch, J.D. and Johnson, D.A. Prototype micro-valve actuator. *Proc. IEEE Micro Electro Mechanical Systems*, Napa Valley, CA, Feb. 11–14, 1990, pp. 40–41.
- [4] Kuribayashi, K., Yoshitake, M. and Ogawa, S. Reversible SMA actuator for micron sized robot. *Proc. IEEE Micro Electro Mechanical Systems*, Napa Valley, CA, Feb. 11–14, 1990, pp. 217–221.
- [5] Hunter, I.W., Lafontaine, S., Nielsen, P.M.F., Hunter, P.J. and Hollerbach, J.M. Manipulation and dynamic mechanical testing of microscopic objects using a tele-micro-robot system. *IEEE Control Systems Magazine*, 1990, 10, 3–9.
- [6] Korenberg, M.J. and Hunter, I.W. The identification of nonlinear biological systems: Wiener kernel approaches. *Annals of Biomedical Engineering*, 1990, in press.
- [7] Korenberg, M.J. and Hunter, I.W. The identification of nonlinear biological systems: Volterra kernel approaches. *Annals of Biomedical Engineering*, 1990, in press.
- [8] Homma, D., Miwa, Y., and Iguchi, N. Micro robots and micro mechanisms using shape memory alloy. *3rd Toyota Conf. Integrated Micro Motion Systems*, Tokyo, Oct. 22–25, 1989, pp. 22–1 – 22–21.
- [9] Ikuta, K. Micro/mimiatuure shape memory alloy actuator. *Proc. IEEE Intl. Conf. Robotics and Automation*, Cincinnati, May 13–18, 1990, pp. 2156–2161.
- [10] Kuribayashi, K. A new actuator of a joint mechanism using TiNi alloy wire. *Int. J. Robotics Research*, 1986, 4, 47–58.